Probing H_2 Double Ionization with Bicircular Laser Fields

Zhenning Guo,[1,*] Zhihe Zhang,[2,*] Yongkai Deng,[1] Jiguo Wang,[1] Difa Ye,[3,†] Jie Liu,[2,4,‡] and Yunquan Liu[1,2,5,§]

[1]State Key Laboratory for Mesoscopic Physics and Frontiers Science Center for Nano-optoelectronics, School of Physics, Peking University, Beijing 100871, China

[2]Center for Applied Physics and Technology, HEDPS, Peking University, Beijing 100871, China

[3]National Key Laboratory of Computational Physics, Institute of Applied Physics and Computational Mathematics, Beijing 100088, China

[4]Graduate School, China Academy of Engineering Physics, Beijing 100193, China

[5]Collaborative Innovation Center of Extreme Optics, Shanxi University, Taiyuan, Shanxi 030006, China

(Received 4 April 2023; revised 30 November 2023; accepted 14 March 2024; published 3 April 2024)

We present a kinematically complete study on strong-field double ionization of H_2 molecules in two-color bicircular laser fields. The releasing times of electrons and protons are recorded with the double-hand attoclock. We observe the relative emission angles of two electrons oscillate with the kinetic energy release of protons, indicating the internal concerted four-body fragmentation. Using a three-dimensional molecular semiclassical ensemble model, we have disentangled the attosecond correlated electron emission in H_2 double ionization. This work reveals the strong electron-nuclear coupling in the molecular bond breaking and may open up a new approach to experimentally accessing the intramolecular electron and bond dynamics with bicircular fields.

DOI: 10.1103/PhysRevLett.132.143201

Measuring and manipulating the internal degrees of freedom in molecules are essential for understanding and steering chemical reactions and biological processes. The introduction of time-resolved pump-probe spectroscopy offers the opportunity to follow the atomic and molecular wave packet dynamics in the time domain and thus has received considerable attention beginning with the pioneering work of Zewail [1]. Since then, numerous studies of molecular fragmentation and isomerization processes that involve vibrations, rotations, and translations have been reported using intense femtosecond laser pulses [2–4], among which the hydrogen molecule H_2 has emerged as a paradigm system [5,6]. For example, tracking the ultrafast vibrational wave packets in H_2 and D_2 has been achieved using near-single-cycle laser pulses [7–9]. More recently, the attosecond community has gradually shifted the attention to much larger molecules [10–13], motivated for instance by the harnessing of ultrafast charge migration and electronic decoherence influenced by nuclear motion in photosynthesis. Specifically, the steering of a molecular nuclear wave packet associated with sub-laser-cycle manipulation of electron dynamics is a subject of significant interest [14–20], leading to the newly emerging field dubbed as "attosecond chemistry" [13,21–24]. One should note, however, that the pump-probe spectroscopy requires two ultrashort light pulses, and the time resolution is limited by the pulse duration.

Additionally, a fascinating approach to probe attosecond electronic dynamics in atoms and molecules is attosecond angular streaking (attoclock) with close-to-circularly polarized fields, in which the ionization instant is mapped onto the final emission angle of the photoelectron [25,26]. Because of its intuitive physical picture and convenient experimental implementation, this technique has been widely used to measure attosecond time-resolved dynamics of electrons and nuclei, such as the tunneling time delay of atomic or molecular photoemission [27–30], and the subcycle nuclear dynamics for double ionization (DI) of H_2 [18,19]. However, due to the upper limit of a single optical cycle (2.6 fs at 800-nm central wavelength) for this traditional attoclock scheme, it is a major obstacle to disentangling the multiperiod emission dynamics of photoelectrons during the slower nuclear motion that takes place on the timescale of tens of femtoseconds. Recently, the corotating circularly polarized (CP) fields have been used to explore the strong-field ionization of atoms and molecules [31–33]. For a chemical reaction triggered by strong laser fields, multiple bursts of photoelectrons are coupled with the ionic motion among molecules and those charged particles move in very different timescales. It is crucial to extract the nuclear motion and, simultaneously, electron dynamics to fully understand the ultrafast chemical reactions.

In this Letter, we demonstrate and implement a novel molecular double-hand clock scheme to study the ionization bursts of photoelectrons with attosecond time resolution in conjunction with tracing the relatively slow nuclear wave packet for strong-field DI of H_2. The complete fragmentation of H_2 was realized with two-color corotating circular fields, which combines the attosecond sensitivity inherent to attoclock (minute hand) with the high

structural sensitivity of Coulomb explosion imaging (hour hand) to probe the coupled motion between the electrons and nuclear wave packets. The essential idea is that the angular offset $\Delta\theta$ between two emitted electrons can be applied to calibrate the time delay Δt between two consecutive ionization bursts, while the molecular bond length R at the instant of DI can be retrieved via the kinetic energy release (KER) of two protons. Therefore, by measuring $\Delta\theta$ as a function of KER, we can actually watch the time evolution of R. With that, we have observed the internal correlation of electrons and ions during the dissociative DI, and can reconstruct the molecular wave packet dynamics in the time domain.

Experimentally, we employ two-color CP laser fields to initiate the DI of H_2 molecules. We use an amplified Ti: sapphire laser that can deliver the laser pulse at 800 nm with a duration of 25 fs at a repetition rate of 3 kHz. The second-harmonic pulse at 400 nm is produced by frequency doubling using a 250-μm-thick β-barium-borate crystal. Then the two-color CP fields are realized from each arm in a Mach-Zehnder interferometer scheme. The peak intensities of the fundamental field and the second-harmonic field are calibrated to be $I_{800} = 8.9 \times 10^{13}$ W/cm^2 and $I_{400} = 5.6 \times 10^{12}$ W/cm^2 using the solution of time-dependent Schrödinger equation of single ionization H_2 [34]. The relative phase between the two-color fields is finely adjusted by using a pair of fused silica wedges. The synthesized bicircular field can be used to clock the DI channel of H_2 ($H_2 \rightarrow H^+ + H^+ + e^- + e^-$), as shown in Fig. 1(a). Here, the instants of the first and second released electrons of DI are clocked with corotating circular fields, which are mapped onto the relative emission angle between these two electrons, constituting the minute hand of the clock. While the hour hand of the clock is represented by the slow motion of dissociative molecular ions, which is reconstructed from the Coulomb explosion of H^+ and H^+. With that, the coupled dynamics of electrons and ions in the dissociative ionization process are fully recorded.

The momenta of protons and electrons were measured via the cold-target recoil-ion reaction momentum spectroscopy [47] in coincidence. The laser pulses were focused with a silver-coated concave mirror ($f = 75$ mm) onto a supersonic gas jet of H_2. The supersonic gas jet was created by expanding H_2 gas into the vacuum through a 30 μm diameter nozzle at a back pressure ~2 bar. A homogeneous static electric field (~4.6 V/cm) and a magnetic field (~6.5 G) were employed to accelerate and guide the ionized ions and electrons to the microchannel plate detectors along the time-of-fight axis. Three-dimensional photoelectron momentum distributions were retrieved from the position and time-of-flight measurements of detectors.

The measured sum energy of two electrons with respect to the KER of DI is shown in Fig. 1(b), and the associated KER distribution is presented in Fig. 2(a) (the solid line). We also measured the relative emission angle of two

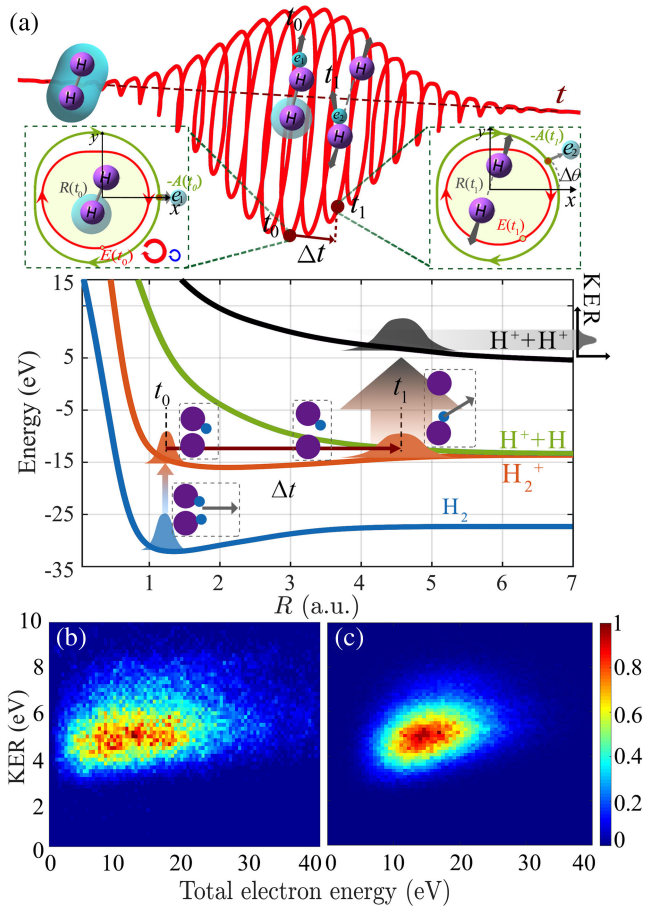

FIG. 1. (a) Scheme of the double-hand clock using bicircular fields for DI of H_2 molecules. When subjected to a bicircular field, the first ionization event at time t_0 initiates near its equilibrium internuclear separation. Then the H_2^+ nuclear wave packet propagates on the vibrational potential energy curve and is finally projected onto the Coulombic potential of $H^+ + H^+$. (b) The measured joint distribution of the sum energy of two photoelectrons and KER of two protons for DI, and (c) the simulated result.

electrons as a function of KER. Here, we note that the momentum of one of the two electrons was measured by an electron detector and the momentum of the other electron was tomographically reconstructed [46]. Interestingly, one can observe a clear signature of oscillation, as seen in Fig. 2(b) (the red dots). As known, the KER of protons is closely related to the molecular internuclear distance. This means that the relative emission angle of two electrons depends on the instantaneous molecular bond length. In the following, together with the simulation results, we will concentrate on how this correlated dynamical system serves as a chronoscope to clock the dissociative process of H_2.

An *ab initio* simulation of the full dynamics of strong-field ionization followed by molecular dissociation and Coulomb explosion is a computationally formidable task at the present time, which is actually a twelve-dimensional multi-timescale problem even for the simplest H_2 molecule

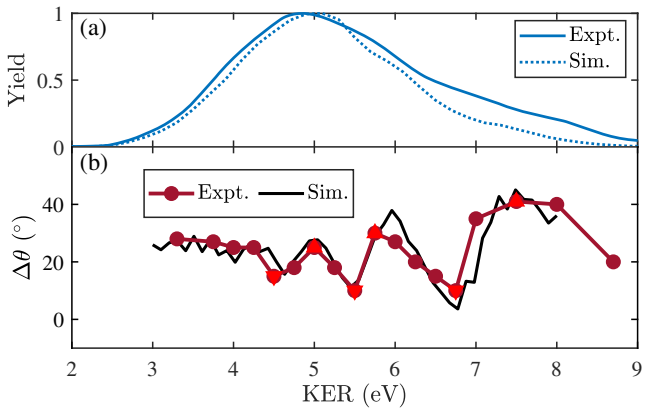

FIG. 2. (a) The measured KER distribution (solid line) and the simulated result (dashed line). (b) The measured KER-dependent angular offset of two electrons (red dots connected with solid line). The up and down triangles mark the peaks and valleys, respectively, calibrating specific KER values. The solid curve shows the corresponding simulation results; see Fig. 3 for further theoretical analysis.

when involving both the electronic and nuclear degrees. We therefore resort to a semiclassical model to understand the physics behind the experimental observations. In our model, one electron is first released by quantum tunneling through the suppressed Coulomb barrier along the negative direction of the laser electric field [48], while the other electron is "instantaneously" promoted to the $1s\sigma_g$ state of H_2^+ with the initial internuclear distance $R_0 = 1.4$ a.u. (the equilibrium distance of H_2), by a vertical excitation according to the Franck-Condon principle [49]. The subsequent evolution of all four particles, including two electrons denoted by $i = 1$ and 2 and two protons denoted by $\mu = a$ and b, are then traced from the tunneling instant to the turn-off of the laser pulse, which is governed by the classical Newton's equations $d^2\mathbf{r}_i/dt^2 = -\boldsymbol{\mathcal{E}}(t) - \nabla_{r_i}(V_{ne} + V_{ee} + V_{\mathrm{KWC}})$, $m_p d^2\mathbf{r}_\mu/dt^2 = \boldsymbol{\mathcal{E}}(t) - \nabla_{r_\mu}(V_{ne} + V_{nn} + V_{\mathrm{KWC}})$, where m_p is the mass of proton, $\boldsymbol{\mathcal{E}}(t)$ is the laser electric field, $V_{ne} = -\sum_{i,\mu} 1/r_{i\mu}$, $V_{ee} = 1/r_{12}$, and $V_{nn} = 1/r_{ab}$ are Coulomb interactions. The extra potential $V_{\mathrm{KWC}} = \sum_{i,\mu}(\xi_H^2/16r_{i\mu}^2)\exp\{4[1-(r_{i\mu}p_{i\mu}/\xi_H)^4]\} + \sum_i(\xi_1^2/16r_{ab}^2)\exp\{4[1-(r_{io}p_{io}/\xi_1)^4]\} + (\xi_2^2/8r_{ab}^2)\exp\{4[1-(r_{12}p_{12}/\xi_2)^4]\}$ is adopted to mimic the Heisenberg uncertainty principle in a classical trajectory Monte Carlo model, as proposed by Kirschbaum, Wilets, Cohen *et. al.* [39,50–52]. Here, $\mathbf{r}$ and $\mathbf{p}$ represent the relative position and momentum between any two particles, and the index o denotes the center of mass of two protons. The parameters take the values of $\xi_H = 0.9428$, $\xi_1 = 0.90$, and $\xi_2 = 1.73$, which are determined by fitting the ground-state energies of H, H_2^+, and H_2 to their experimental values. This gives almost identical molecular potential energy curves with quantum-mechanical calculations [39], ensuring that some key processes essential to the understanding of dissociative DI, such as the spread of molecular wave packet or even the anharmonic oscillations in between the turning points, are correctly captured in our semiclassical simulations [34].

We exploit the semiclassical model to calculate the joint distribution of the KER and the sum energy of two electrons, as shown in Fig. 1(c), which agrees with the experimental measurements in broad terms. It can be concluded that the dynamics under investigation are mainly classical so we can take full advantage of the classical trajectory Monte Carlo approach to explore the underlying physics behind the experimental observations. To make a more quantitative comparison, we then integrate the spectra over the electron energy and get the KER distributions. As can be seen from Fig. 2(a), an almost quantitative agreement is reached between experiment and theory: both show the maximal distribution at KER ≈ 5 eV. Presumably, most of the DI events take place when the molecule stretches to a bond length $R \approx 1/\mathrm{KER} \approx 5.4$ a.u. As a result, the real-time observation of the electron-nucleus-coupled DI dynamics can not be accomplished with the traditional molecular clocks [14,18], which can only make a "molecular movie" within the first few femtoseconds and typically with $R < 3$ a.u. Below we will propose a novel double-hand molecular clock by taking advantage of the KER-dependent oscillation of the relative emission angle between two electrons (KOREA).

Time zero.—In our scheme, the clock starts ticking when the first electron is released from the molecule. This occurs most probably at the local field maximums according to the Ammosov-Delone-Krainov theory, as seen in Fig. 3(a) (blue curve) [34]. The first electron always tends to be emitted into a specific direction near −20° [see Fig. 3(b)], regardless of the KER measured in the final state. This most probable emission angle is associated with the direction of the maximal vector potential and is further affected by the ionic potential. The deviation from 0° is due to the Coulomb scattering, which has been intensively investigated in the conventional attoclock scheme [53–55]. The almost constant behavior of the emission angle allows us to set it as an angular or, equivalently, time reference to clock the subsequent ionization and dissociation processes.

The minute hand and the hour hand.—By contrast, the emission angle of the second released electron oscillates notably with KER [see Fig. 3(c)], in a nearly opposite trend against the KOREA. This contains the vital information on ionization and dissociation dynamics. With the increase of KER, the second electrons are periodically released into a specific direction from −180° to 180°, as indicated by the three streaks marked by white dashed lines with decreasing slopes. The location of these streaks is closely related to the peaks and valleys on the KOREA (green solid line). This reveals the underlying mechanism for the oscillation behavior in the KOREA. In fact, the streaks imply that the emission angle of the second electron rotates together with the instantaneous electric field, and each streak

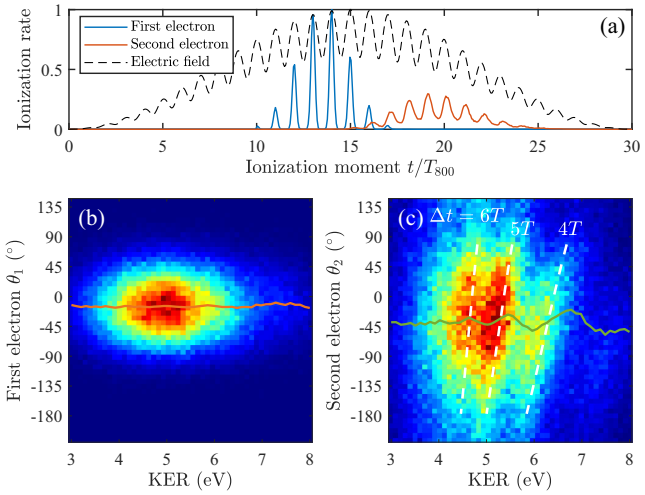

FIG. 3. Theoretical analysis of the KOREA by tracing the two electrons individually, which is possible only in simulations since the two electrons are identical in experiment. (a) Ionization bursts of two electrons (solid lines) in the DI channel. The dashed line indicates the instantaneous electric field strength. (b) and (c) are the emission angles of two electrons versus KER. The three dashed white lines mark the streaks corresponding to ionization time delays $\Delta t = 4T$, $5T$, and $6T$, respectively. The orange line in (b) and green line in (c) represent the averaged value of emission angle at different KERs.

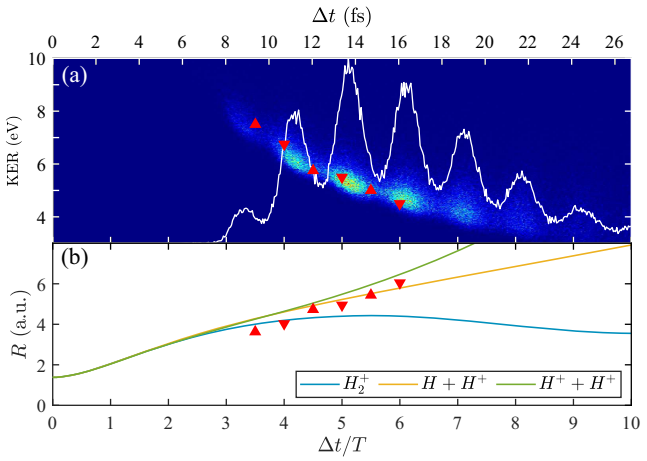

FIG. 4. (a) The contour plot shows the simulated KER distributions at different time delays Δt, which provides a KER-to-time mapping relationship for retrieving the temporal information related to the peaks and valleys in the KOREA. In this way, the horizontal and vertical coordinates of the triangles are determined: while the KER values are extracted from the experimentally observed KOREA, the corresponding values of Δt are inferred from the contour plot. The white solid curve represents the distribution of Δt. (b) The evolution of averaged R for different ionization and dissociation channels (colored lines). The triangles are retrieved using the relation $R(\Delta t) = 1/\mathrm{KER}(\Delta t)$.

corresponds to a single field cycle. Thus we can see that being different from the first electron, the second electron is ionized more uniformly over each single field cycle, not only near the maximal electric field. In Fig. 3(a), we have analyzed the ionization rate of the second electrons, and there is still considerable ionization probability at the local field minimums. Such a character allows us to take advantage of the emission angle of the second electron to serve as the minute hand, calibrating the finer time in a single period.

The relatively slow proton dynamics, associated with the KER spectrum, can serve as the hour hand of the molecular clock. The KER distribution at different Δt (the ionization time delay between two electrons) is shown in Fig. 4(a). The white solid line represents the probability distribution of Δt. The time-resolved result of KER reveals apparent structures. Here, we can see those events with $\Delta t = 4T$, $5T$, and $6T$ give the main contribution, and each period of Δt links to different regions of KER clearly. Therefore, it is feasible to establish the KER-to-time mapping relation, serving as the hour hand.

We would like to mention that, for a multicycle single circular field, the oscillations of KOREA would fade away [34]. Thus the application of a bicircular field is crucial to break the symmetry and to set up the molecular clock.

Application of the double-hand molecular clock.—Having explained the components of a clock, we now revisit the experimentally observed KOREA and show how the molecular clock can be applied to trace the long-term evolution of the molecular wave packet along the potential energy curve. According to the above theoretical time-resolved KER analysis [contour plot in Fig. 4(a)], we can estimate that the location of the three peaks (up triangles) in Fig. 2(b) calibrate half-integral periods of Δt and the three valleys (down triangles) calibrate integral periods of Δt. The KER is naturally associated with two-body Coulomb explosion, which can be used to track the proton motion in H_2^+. We plot the retrieved internuclear distance with respect to the time delay of two electrons in Fig. 4(b) (triangles). Using semiclassical simulation, we also analyze the internuclear distance evolution for the dissociative single ionization and DI (colored lines). One can see that, in the two-color bicircular field, the molecule is promoted to the $1s\sigma_g$ state right after the emission of the first electron at the time zero (i.e., $\Delta t = 0$ fs, $R = 1.4$ a.u.), coupled with the $2p\sigma_u$ state at $\Delta t \approx 7$ fs ($R \approx 3.5$ a.u.), and then starts to dissociate accompanying with the emission of the second electron at $\Delta t \approx 13$ fs ($R \approx 5$ a.u.). In the above process, the emission of the second electron probes the motion of cores at different time delays. The divergence between the triangles and the green line ($H^+ + H^+$ channel) is due to the inaccuracy of $R(\Delta t) = 1/\mathrm{KER}(\Delta t)$, in which the zero initial velocity of proton at dissociation moment was assumed [56]. The underestimation of core initial velocity leads to lower internuclear distance R. In general, our reconstruction of the molecular dynamics proves that the most probable dissociation internuclear distance is around 5 a.u. [as evidenced by Figs. 4(a) and 4(b)], which can be regarded as direct evidence of the charge-resonance-enhanced ionization [57–60].

In conclusion, we have explored the strong-field double ionization of H_2 molecules with corotating two-color circular fields. The correlated dynamics of two-electron and two-proton among the molecules have been decoupled with the novel clocking geometry. The emission angle of electrons denotes the specific dissociative moment in a laser cycle, serving as the minute hand in the molecular clock. Meanwhile, the KER-resolved motion of protons makes it possible to demarcate between different cycles, serving as the hour hand. The oscillation of the relative emission angle between two electrons with respect to KER clearly indicates the internal coupling in the dissociation process. The bicircular laser fields can be readily extended to clock the fragmentation of other diatomic and polyatomic molecules with many-particle coincidence measurement.

This work was supported by the National Key R&D Program of China (2022YFA1604301 and 2023YFA1406803), the National Natural Science Foundation of China (NSFC) (Grants No. 92050201, No. 92250306, No. 12174034, and No. 12334013), and NSAF (Grant No. U2330401).

*These authors contributed equally to this letter.
†Corresponding author: ye_difa@iapcm.ac.cn
‡Corresponding author: jliu@gscaep.ac.cn
§Corresponding author: yunquan.liu@pku.edu.cn

[1] A. H. Zewail, Laser femtochemistry, Science **242**, 1645 (1988).
[2] J. H. Posthumus, The dynamics of small molecules in intense laser fields, Rep. Prog. Phys. **67**, 623 (2004).
[3] I. V. Hertel and W. Radloff, Ultrafast dynamics in isolated molecules and molecular clusters, Rep. Prog. Phys. **69**, 1897 (2006).
[4] J. Xu, C. I. Blaga, P. Agostini, and L. F. DiMauro, Time-resolved molecular imaging, J. Phys. B **49**, 112001 (2016).
[5] C. R. Calvert, W. A. Bryan, W. R. Newell, and I. D. Williams, Time-resolved studies of ultrafast wave-packet dynamics in hydrogen molecules, Phys. Rep. **491**, 1 (2010).
[6] H. Ibrahim, C. Lefebvre, A. D. Bandrauk, A. Staudte, and F. Légaré, H2: The benchmark molecule for ultrafast science and technologies, J. Phys. B **51**, 042002 (2018).
[7] T. Ergler, A. Rudenko, B. Feuerstein, K. Zrost, C. D. Schröter, R. Moshammer, and J. Ullrich, Spatiotemporal imaging of ultrafast molecular motion: Collapse and revival of the D_2^+ nuclear wave packet, Phys. Rev. Lett. **97**, 193001 (2006).
[8] A. S. Alnaser, B. Ulrich, X. M. Tong, I. V. Litvinyuk, C. M. Maharjan, P. Ranitovic, T. Osipov, R. Ali, S. Ghimire, Z. Chang, C. D. Lin, and C. L. Cocke, Simultaneous real-time tracking of wave packets evolving on two different potential curves in H_2^+ and D_2^+, Phys. Rev. A **72**, 030702(R) (2005).
[9] H. Niikura, D. M. Villeneuve, and P. B. Corkum, Controlling vibrational wave packets with intense, few-cycle laser pulses, Phys. Rev. A **73**, 021402(R) (2006).
[10] A. Trabattoni, M. Klinker, J. González-Vázquez, C. Liu, G. Sansone, R. Linguerri, M. Hochlaf, J. Klei, M. J. J. Vrakking, F. Martín, M. Nisoli, and F. Calegari, Mapping the dissociative ionization dynamics of molecular nitrogen with attosecond time resolution, Phys. Rev. X **5**, 041053 (2015).
[11] F. Calegari, D. Ayuso, A. Trabattoni, L. Belshaw, S. DE Camillis, S. Anumula, F. Frassetto, L. Poletto, A. Palacios, P. Decleva, J. B. Greenwood, F. Martín, and M. Niosli, Ultrafast electron dynamics in phenylalanine initiated by attosecond pulses, Science **346**, 336 (2014).
[12] C. Arnold, O. Vendrell, and R. Santra, Electronic decoherence following photoionization: Full quantum-dynamical treatment of the influence of nuclear motion, Phys. Rev. A **95**, 033425 (2017).
[13] C. Arnold, O. Vendrell, R. Welsch, and R. Santra, Control of nuclear dynamics through conical intersections and electronic coherences, Phys. Rev. Lett. **120**, 123001 (2018).
[14] H. Niikura, F. Légaré, R. Hasbani, M. Y. Ivanov, D. M. Villeneuve, and P. B. Corkum, Probing molecular dynamics with attosecond resolution using correlated wave packet pairs, Nature (London) **421**, 826 (2003).
[15] M. F. Kling, C. Siedschlag, A. J. Verhoef, J. I. Khan, M. Schultze, T. Uphues, Y. Ni, M. Uiberacker, M. Drescher, F. Krausz, and M. J. J. Vrakking, Control of electron localization in molecular dissociation, Science **312**, 246 (2006).
[16] G. Sansone *et al.*, Electron localization following attosecond molecular photoionization, Nature (London) **465**, 763 (2010).
[17] L. Cattaneo, J. Vos, R. Bello, A. Palacios, S. Heuser, L. Pedrelli, M. Lucchini, C. Cirelli, F. Martín, and U. Keller, Attosecond coupled electron and nuclear dynamics in dissociative ionization of H_2, Nat. Phys. **14**, 733 (2018).
[18] V. Hanus, S. Kangaparambil, S. Larimian, M. Dorner-Kirchner, X. Xie, M. S. Schöffler, G. G. Paulus, A. Baltuška, A. Staudte, and M. Kitzler-Zeiler, Subfemtosecond tracing of molecular dynamics during strong-field interaction, Phys. Rev. Lett. **123**, 263201 (2019).
[19] V. Hanus, S. Kangaparambil, S. Larimian, M. Dorner-Kirchner, X. Xie, M. S. Schöffler, G. G. Paulus, A. Baltuška, A. Staudte, and M. Kitzler-Zeiler, Experimental separation of subcycle ionization bursts in strong-field double ionization of H_2, Phys. Rev. Lett. **124**, 103201 (2020).
[20] S. Pan, W. Zhang, H. Li, C. Lu, W. Zhang, Q. Ji, H. Li, F. Sun, J. Qiang, F. Chen, J. Tong, L. Zhou, W. Jiang, X. Gong, P. Lu, and J. Wu, Clocking dissociative above-threshold double ionization of H_2 in a multicycle laser pulse, Phys. Rev. Lett. **126**, 063201 (2021).
[21] F. Krausz and M. Ivanov, Attosecond physics, Rev. Mod. Phys. **81**, 163 (2009).
[22] F. Lépine, M. Ivanov, and M. Vrakking, Attosecond molecular dynamics: Fact or fiction?, Nat. Photonics **8**, 195 (2014).
[23] M. Nisoli, P. Decleva, F. Calegari, A. Palacios, and F. Martín, Attosecond electron dynamics in molecules, Chem. Rev. **117**, 10760 (2017).

[24] A. Palacios and F. Martín, The quantum chemistry of attosecond molecular science, WIREs Comput. Mol. Sci. **10**, e1430 (2020).

[25] P. Eckle, M. Smolarski, P. Schlup, J. Biegert, A. Staudte, M. Schöffler, H. Muller, R. Dörner, and U. Keller, Attosecond angular streaking, Nat. Phys. **4**, 565 (2008).

[26] P. Eckle, A. N. Pfeiffer, C. Cirelli, A. Staudte, R. Dörner, H. G. Muller, M. Büttiker, and U. Keller, Attosecond ionization and tunneling delay time measurements in helium, Science **322**, 1525 (2008).

[27] C. Cirelli, M. Smolarski, M. Abu-samha, L. Madsen, U. Keller, A. Pfeiffer, and D. Dimitrovski, Attoclock reveals natural coordinates of the laser-induced tunnelling current flow in atoms, Nat. Phys. **8**, 76 (2011).

[28] A. S. Landsman, M. Weger, J. Maurer, R. Boge, A. Ludwig, S. Heuser, C. Cirelli, L. Gallmann, and U. Keller, Ultrafast resolution of tunneling delay time, Optica **1**, 343 (2014).

[29] U. S. Sainadh, H. Xu, X. Wang, A. Atia-tul Noor, W. C. Wallace, N. Douguet, A. Bray, I. Ivanov, K. Bartschat, A. Kheifets, R. T. Sang, and I. V. Litvinyuk, Attosecond angular streaking and tunnelling time in atomic hydrogen, Nature (London) **568**, 75 (2019).

[30] W. Quan, V. V. Serov, M. Z. Wei, M. Zhao, Y. Zhou, Y. L. Wang, X. Y. Lai, A. S. Kheifets, and X. J. Liu, Attosecond molecular angular streaking with all-ionic fragments detection, Phys. Rev. Lett. **123**, 223204 (2019).

[31] M. Han, P. Ge, Y. Shao, Q. Gong, and Y. Liu, Attoclock photoelectron interferometry with two-color corotating circular fields to probe the phase and the amplitude of emitting wave packets, Phys. Rev. Lett. **120**, 073202 (2018).

[32] Z. Guo, Y. Fang, P. Ge, X. Yu, J. Wang, M. Han, Q. Gong, and Y. Liu, Probing tunneling dynamics of dissociative H_2 molecules using two-color bicircularly polarized fields, Phys. Rev. A **104**, L051101 (2021).

[33] Z. Guo, P. Ge, Y. Fang, Y. Dou, X. Yu, J. Wang, Q. Gong, and Y. Liu, Probing molecular frame Wigner time delay and electron wavepacket phase structure of CO molecule, Ultrafast Sci. **2022**, 9802917 (2022).

[34] See Supplemental Material at http://link.aps.org/supplemental/10.1103/PhysRevLett.132.143201 for more details on the molecular semiclassical model, some numerical simulations based on the time-dependent Schrödinger equation, the laser intensity calibration method, procedure for the extraction of the relative emission angle between two electrons in experiment, the two-electron sum-energy spectra, and numerical results with a single-color circularly polarized laser pulse, which includes Refs. [35–46].

[35] M. Peters, T. T. Nguyen-Dang, E. Charron, A. Keller, and O. Atabek, Laser-induced electron diffraction: A tool for molecular orbital imaging, Phys. Rev. A **85**, 053417 (2012).

[36] M.-M. Liu, M. Han, P. Ge, C. He, Q. Gong, and Y. Liu, Strong-field ionization of diatomic molecules in orthogonally polarized two-color fields, Phys. Rev. A **97**, 063416 (2018).

[37] M. D. Feit, J. A. Fleck, and A. Steiger, Solution of the Schrödinger equation by a spectral method, J. Comput. Phys. **47**, 412 (1982).

[38] J. Liu, *Classical Trajectory Perspective of Atomic Ionization in Strong Laser Fields: Semiclassical Modeling* (Springer, Heidelberg, 2014).

[39] J. S. Cohen, Molecular effects on antiproton capture by H_2 and the states of $\bar{p}p$ formed, Phys. Rev. A **56**, 3583 (1997).

[40] M. V. Ammosov, N. B. Delone, and V. P. Krainov, Tunnel ionization of complex atoms and of atomic ions in an alternating electromagnetic field, Sov. Phys. JETP **64**, 1191 (1986).

[41] L. D. Landau and E. M. Lifshitz, *Quantum Mechanics: Non-Relativistic Theory* (Pergamon Press, New York, 1977).

[42] W. H. Press, B. P. Flannery, S. A. Teukolsky, and W. T. Vetterling, *Numerical Recipes in FORTRAN: The Art of Scientific Computing* (Cambridge University Press, Cambridge, England, 1992).

[43] J. S. Cohen, Comment on the classical-trajectory Monte Carlo method for ion-atom collisions, Phys. Rev. A **26**, 3008 (1982).

[44] D. F. Ye, X. Liu, and J. Liu, Classical trajectory diagnosis of a fingerlike pattern in the correlated electron momentum distribution in strong field double ionization of helium, Phys. Rev. Lett. **101**, 233003 (2008).

[45] P. Wang, A. M. Sayler, K. D. Carnes, B. D. Esry, and I. Ben-Itzhak, Disentangling the volume effect through intensity-difference spectra: Application to laser-induced dissociation of H_2^+, Opt. Lett. **30**, 664 (2005).

[46] S. Eckart, M. Richter, M. Kunitski, A. Hartung, J. Rist, K. Henrichs, N. Schlott, H. Kang, T. Bauer, H. Sann, L. Ph. H. Schmidt, M. Schöffler, T. Jahnke, and R. Dörner, Nonsequential double ionization by counterrotating circularly polarized two-color laser fields, Phys. Rev. Lett. **117**, 133202 (2016).

[47] J. Ullrich, R. Moshammer, A. Dorn, R. Dörner, L. P. H. Schmidt, and H. Schmidt-Böcking, Recoil-ion and electron momentum spectroscopy: Reaction-microscopes, Rep. Prog. Phys. **66**, 1463 (2003).

[48] Hong Liu, Yunquan Liu, Libin Fu, Guoguo Xin, Difa Ye, Jie Liu, X. T. He, Yudong Yang, Xianrong Liu, Yongkai Deng, Chengyin Wu, and Qihuang Gong, Low yield of near-zero-momentum electrons and partial atomic stabilization in strong-field tunneling ionization, Phys. Rev. Lett. **109**, 093001 (2012).

[49] H. Niikura, F. Légaré, R. Hasbani, A. Bandrauk, M. Y. Ivanov, D. Villeneuve, and P. Corkum, Sub-laser-cycle electron pulses for probing molecular dynamics, Nature (London) **417**, 917 (2002).

[50] C. L. Kirschbaum and L. Wilets, Classical many-body model for atomic collisions incorporating the Heisenberg and Pauli principles, Phys. Rev. A **21**, 834 (1980).

[51] K. J. LaGattuta, Behavior of H_2^+ and H_2 in strong laser fields simulated by fermion molecular dynamics, Phys. Rev. A **73**, 043404 (2006).

[52] E. Lötstedt, T. Kato, and K. Yamanouchi, Classical dynamics of laser-driven D_3^+, Phys. Rev. Lett. **106**, 203001 (2011).

[53] L. Torlina, F. Morales, J. Kaushal, H. Muller, I. Ivanov, A. Kheifets, A. Zielinski, A. Scrinzi, M. Ivanov, and O. Smirnova, Interpreting attoclock measurements of tunnelling times, Nat. Phys. **11**, 503 (2014).

[54] M. Han, P. Ge, Y. Fang, X. Yu, Z. Guo, X. Ma, Y. Deng, Q. Gong, and Y. Liu, Unifying tunneling pictures of strong-field ionization with an improved attoclock, Phys. Rev. Lett. **123**, 073201 (2019).

[55] J. Yuan, S. Liu, X. Wang, Z. Shen, Y. Ma, H. Ma, Q. Meng, T.-M. Yan, Y. Zhang, A. Dorn, M. Weidemüller, D. Ye, and Y. Jiang, Ellipticity-dependent sequential over-barrier ionization of cold rubidium, Phys. Rev. A **102**, 043112 (2020).

[56] H. Xu, Z. Li, F. He, X. Wang, A. Atia-Tul-Noor, D. Kielpinski, R. Sang, and I. Litvinyuk, Observing electron localization in a dissociating H_2^+ molecule in real time, Nat. Commun. **8**, 15849 (2017).

[57] T. Zuo and A. D. Bandrauk, Charge-resonance-enhanced ionization of diatomic molecular ions by intense lasers, Phys. Rev. A **52**, R2511 (1995).

[58] I. Ben-Itzhak, P. Q. Wang, A. M. Sayler, K. D. Carnes, M. Leonard, B. D. Esry, A. S. Alnaser, B. Ulrich, X. M. Tong, I. V. Litvinyuk, C. M. Maharjan, P. Ranitovic, T. Osipov, S. Ghimire, Z. Chang, and C. L. Cocke, Elusive enhanced ionization structure for H_2^+ in intense ultrashort laser pulses, Phys. Rev. A **78**, 063419 (2008).

[59] Y. Mi, P. Peng, N. Camus, X. Sun, P. Fross, D. Martinez, Z. Dube, P. B. Corkum, D. M. Villeneuve, A. Staudte, R. Moshammer, and T. Pfeifer, Clocking enhanced ionization of hydrogen molecules with rotational wave packets, Phys. Rev. Lett. **125**, 173201 (2020).

[60] K. Liu and I. Barth, Distinguishing two mechanisms for enhanced ionization of H_2^+ using orthogonal two-color laser fields, Phys. Rev. A **103**, 013103 (2021).